Analyst

TUTORIAL REVIEW

View Article Online
View Journal | View Issue

Open Access Article. Published on 03 November 2015. Downloaded on 22/07/2016 16:53:49.
This article is licensed under a Creative Commons Attribution-NonCommercial 3.0 Unported Licence.

Cite this: *Analyst*, 2016, **141**, 62

Considering the chemical energy requirements of the tri-*n*-propylamine co-reactant pathways for the judicious design of new electrogenerated chemiluminescence detection systems†

Emily Kerr,[a] Egan H. Doeven,[b] David J. D. Wilson,[c] Conor F. Hogan[c] and Paul S. Francis*[a]

Received 19th July 2015,
Accepted 8th October 2015

DOI: 10.1039/c5an01462j

www.rsc.org/analyst

The introduction of a 'co-reactant' was a critical step in the evolution of electrogenerated chemiluminescence (ECL) from a laboratory curiosity to a widely utilised detection system. In conjunction with a suitable electrochemiluminophore, the co-reactant enables generation of both the oxidised and reduced precursors to the emitting species at a single electrode potential, under the aqueous conditions required for most analytical applications. The most commonly used co-reactant is tri-*n*-propylamine (TPrA), which was developed for the classic tris(2,2′-bipyridine)ruthenium(II) ECL reagent. New electrochemiluminophores such as cyclometalated iridium(III) complexes are also evaluated with this co-reactant. However, attaining the excited states in these systems can require much greater energy than that of tris(2,2′-bipyridine)ruthenium(II), which has implications for the co-reactant reaction pathways. In this tutorial review, we describe a simple graphical approach to characterise the energetically feasible ECL pathways with TPrA, as a useful tool for the development of new ECL detection systems.

Early electrogenerated chemiluminescence (ECL) experiments involved the electrochemical oxidation and reduction of a luminescent compound to form reactive radicals capable of generating the radiative electronically excited state through annihilation (reactions (1)–(4)).[1]

$$M - e^- \rightarrow M^+ \quad \text{(oxidation during anodic step)} \qquad (1)$$

$$M + e^- \rightarrow M^- \quad \text{(reduction during cathodic step)} \qquad (2)$$

$$M^+ + M^- \rightarrow M^* + M \quad \text{(excited state formation)} \qquad (3)$$

$$M^* \rightarrow M + h\nu \quad \text{(emission of light)} \qquad (4)$$

Although this process remains important for the exploration of the fundamental properties of ECL systems[2–4] and the development of ECL-based light-emitting devices,[5] its application in chemical analysis is limited by the relatively small potential window of aqueous solutions, which generally prohibits the direct electrochemical generation of both the oxidised and reduced species. An elegant solution to this problem was devised by Bard and co-workers,[6,7] who utilised oxalate as a 'co-reactant' that when oxidised, forms a strong reductant ($CO_2^{-\bullet}$). Thus, a water-soluble luminophore such as tris(2,2′-bipyridine)-ruthenium(II) ($[Ru(bpy)_3]^{2+}$) could be oxidised in the presence of oxalate, with the subsequent reaction between $[Ru(bpy)_3]^{3+}$ and $CO_2^{-\bullet}$ generating the radiative excited state (reactions (5)–(7)).[7]

$$[Ru(bpy)_3]^{2+} - e^- \rightarrow [Ru(bpy)_3]^{3+} \qquad (5)$$

$$[Ru(bpy)_3]^{3+} + C_2O_4^{2-} \rightarrow [Ru(bpy)_3]^{2+} + CO_2^{-\bullet} + CO_2 \qquad (6)$$

$$[Ru(bpy)_3]^{3+} + CO_2^{-\bullet} \rightarrow [Ru(bpy)_3]^{2+*} + CO_2 \qquad (7)$$

Leland and Powell[8] subsequently demonstrated that tri-*n*-propylamine (TPrA) was an even more effective co-reactant for $[Ru(bpy)_3]^{2+}$ ECL. Oxidation of TPrA and related amines initially produces the corresponding aminium radical cation, which rapidly deprotonates to form a highly reductive α-amino alkyl radical (reactions (8) and (9)).

$$TPrA - e^- \rightarrow TPrA^{+\bullet} \qquad (8)$$

$$TPrA^{+\bullet} \rightarrow TPrA^{\bullet} + H^+ \qquad (9)$$

A vast range of ECL-based analytical applications involving $[Ru(bpy)_3]^{2+}$ (and its derivatives) with TPrA as co-reactant have

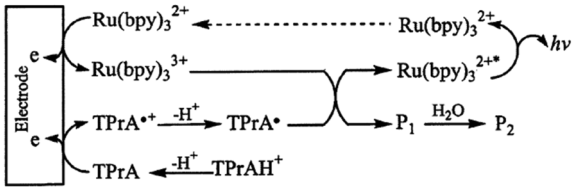
[a]Centre for Chemistry and Biotechnology, School of Life and Environmental Sciences, Faculty of Science, Engineering and Built Environment, Deakin University, Geelong, Victoria 3220, Australia. E-mail: paul.francis@deakin.edu.au
[b]Centre for Rural and Regional Futures, School of Life and Environmental Sciences, Faculty of Science, Engineering and Built Environment, Deakin University, Geelong, Victoria 3220, Australia
[c]Department of Chemistry and Physics, La Trobe Institute for Molecular Science, La Trobe University, Melbourne, Victoria 3086, Australia

†Electronic supplementary information (ESI) available. See DOI: 10.1039/c5an01462j

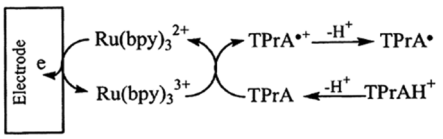
This journal is © The Royal Society of Chemistry 2016

Open Access Article. Published on 03 November 2015. Downloaded on 22/07/2016 16:53:49.
This article is licensed under a Creative Commons Attribution-NonCommercial 3.0 Unported Licence.

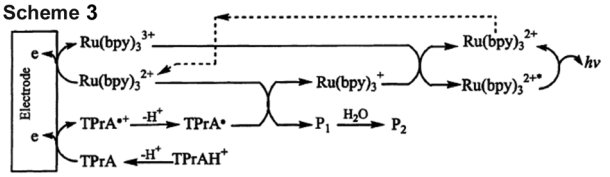
Scheme 1



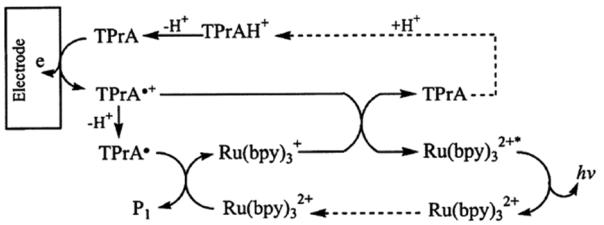
Scheme 2



Scheme 3



Scheme 4



Schemes 1–4 The mechanism of co-reactant ECL for $[Ru(bpy)_3]^{2+}$ and TPrA. Adapted from W. Miao, J.-P. Choi, and A. J. Bard, Electrogenerated chemiluminescence 69: the tris(2,2′-bipyridine)ruthenium(II), $(Ru(bpy)_3^{2+})$/tri-*n*-propylamine (TPrA) system revisited – a new route involving TPrA cation radicals, *J. Am. Chem. Soc.*, **124**, 14478–14485. Copyright 2002, American Chemical Society.

since emerged,[9,10] and the reaction mechanism has been extensively explored.[8,11–14]

In 2002, Bard and co-workers[13] provided a comprehensive account of the light-producing reaction pathways of the $[Ru(bpy)_3]^{2+}$-TPrA ECL system (Schemes 1–3), and uncovered an additional route (Scheme 4) that reconciled several seemingly anomalous previous findings. This work has been recounted in the literature on many occasions,[9,15] and (at least in part) extended to describe related ECL systems involving other metal complexes or alternative co-reactants.[3,14,16–18]

The relative contribution from each pathway of Schemes 1–4 is influenced by the reaction conditions, and fundamentally dependent on the relative redox potentials of each species in solution. This is an important consideration in the design of novel co-reactants and electrochemiluminophores, particularly those with emission wavelengths that can vary greatly from those of $[Ru(bpy)_3]^{2+}$.

Cyclometalated Ir^{III} complexes are currently of great interest for the development of reagents with superior ECL efficiencies and emission colours that span the entire visible spectrum.[9,19,20] These complexes offer not only improvements in the analytical performance of existing ECL methodology,[17,21] but also the possibility of multi-colour, multiplexed ECL assays.[22–25] However, the generation of the excited states in these systems can require significantly greater energy than that of $[Ru(bpy)_3]^{2+}$*, which has important implications for the contribution (and even the feasibility) of the pathways shown in Schemes 1–4. Herein, we re-examine the classic co-reactant ECL discussion of Bard and co-workers[13] under the new context of Ir^{III}-based multi-coloured ECL. We then discuss the limitations of considering the reactions in this manner.

Schemes 1–4 can be summarised (and generalised) as the following key reaction steps:

$$M - e^- \rightarrow M^+ \quad (10)$$

$$TPrA - e^- \rightarrow TPrA^{+\bullet} \quad (11)$$

$$M^+ + TPrA \rightarrow M + TPrA^{+\bullet} \quad (12)$$

$$TPrA^{+\bullet} \rightarrow TPrA^{\bullet} + H^+ \quad (13)$$

$$M^+ + TPrA^{\bullet} \rightarrow M^* + \text{other products} \quad (14)$$

$$M + TPrA^{\bullet} \rightarrow M^- + \text{other products} \quad (15)$$

$$M^- + M^+ \rightarrow M^* + M \quad (16)$$

$$M^- + TPrA^{+\bullet} \rightarrow M^* + TPrA \quad (17)$$

$$M^* \rightarrow M + h\nu \quad (18)$$

In our initial discussion, we compare the energy requirements of the key reaction steps of each scheme with the emission wavelengths and redox potentials of $[Ru(bpy)_3]^{2+}$ and four Ir^{III} complexes examined in previous ECL studies: $[Ir(ppy)_2(phen)]^+$ (phen = 1,10-phenanthroline),[17,26] $[Ir(ppy)_3]$ (ppy = 2-phenylpyridine),[4,17,18,22,23] $[Ir(df\text{-}ppy)_3]$ (df-ppy = difluoro-2-phenylpyridine),[4,18,24] and $[Ir(df\text{-}ppy)_2(ptb)]^+$ (ptb = 1-benzyl-1,2,3-triazol-4-ylpyridine).[4,18] These complexes have been reported to generate co-reactant ECL intensities with TPrA that were 400%, 1.4%, 7.2% and 24% that of $[Ru(bpy)_3]^{2+}$, respectively, in acetonitrile.[17,18] We have also included $[Ir(pmi)_3]$,[4,18] which has a high photoluminescence quantum efficiency, but does not exhibit co-reactant ECL with TPrA. Most of these complexes are not soluble in water, but they have formed the basis of further development of Ir^{III} complexes exhibiting high ECL efficiencies and/or water solubility. We have therefore used their properties measured in acetonitrile. It is not ideal to compare redox potentials measured in different solvents,[27] but similar potentials have been reported for the oxidation of TPrA in water (0.88 V *vs.* SCE)[12,28] and acetonitrile/benzene (0.9 V *vs.* SCE).[28] Moreover, a $TPrA^{\bullet}$ reduction potential of −1.7 V (*vs.* SCE) has been used to estimate the energetics of ECL reactions in aqueous and non-aqueous solvents.[13,28]

When considering Scheme 1 (incorporating reactions (10), (11), (13), (14) and (18)) in the development of a new metal complex, M, the energy required to generate the excited state

Open Access Article. Published on 03 November 2015. Downloaded on 22/07/2016 16:53:49.
This article is licensed under a Creative Commons Attribution-NonCommercial 3.0 Unported Licence.

M* (*via* reaction (14)) will be greater when the wavelength of emission is shorter ($E = hc/\lambda$). In a previous study, Kapturkiewicz and Angulo[21] explored the influence of energetics on ECL efficiency for the case of varying reduction potential and constant E°_{ox}. More recently, Hogan and co-workers[29] proposed a plot of E°_{ox} *versus* λ_{max} of the metal complex (luminophore) as a means of quickly identifying energy sufficient co-reactant ECL systems (with constant co-reactant reduction potential). Referred to as the 'wall of energy sufficiency', the plot suggests critical values of E°_{ox} for each emission wavelength, which can be estimated from the requirement of a favourable free energy ($\Delta G < 0$) of the electron transfer reaction (reaction (14)):

$$\Delta G = E^{\circ}(\mathrm{TPrA}^{\bullet}) - E^{\circ}_{ox} + E_{ES} \qquad (19)$$

where E_{ES} is the spectroscopic energy of the excited state (in eV) and $E^{\circ}(\mathrm{TPrA}^{\bullet})$ is the reduction potential of the $\mathrm{TPrA}^{\bullet}$ radical. The E_{ES} is ideally taken from the λ_{max} of the emission spectrum measured at low temperature, but can be derived from room-temperature data to a first approximation. For simplicity, we have omitted the Coulomb repulsion energy required to bring the reactants into the active complex and the vibrational levels of the radiative transition, as these contributions are relatively small. For analytical applications of ECL, the analysis of Hogan and co-workers[29] is most relevant, where the emission colour and oxidative power of the luminophore are the variables, and the reduction potential of the co-reactant is constant.

The utility of this analysis is illustrated in Fig. 1 with a plot of energy requirements for Scheme 1 with a TPrA co-reactant.

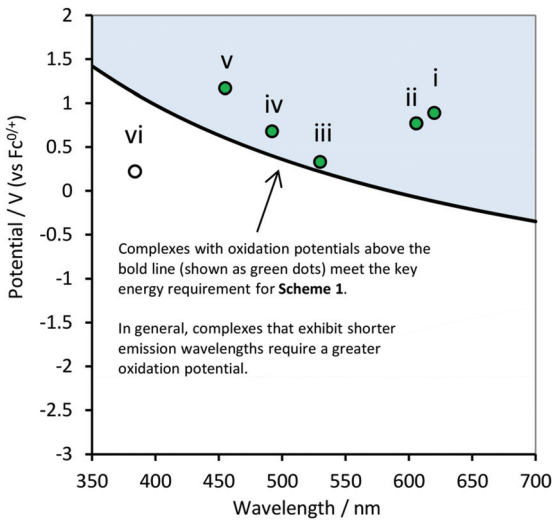


Fig. 1 Energy requirements for Scheme 1 (reaction (14)) with TPrA as co-reactant, in terms of oxidation potentials and emission wavelengths of the metal complexes: (i) $[Ru(bpy)_3]^{2+}$, (ii) $[Ir(ppy)_2(phen)]^{+}$, (iii) $[Ir(ppy)_3]$, (iv) $[Ir(df\text{-}ppy)_3]$, (v) $[Ir(df\text{-}ppy)_2(ptb)]^{+}$, and (vi) $[Ir(pmi)_3]$. Reaction (14) is energetically favourable for complexes with oxidation potentials above the line (in the blue coloured area). The curved line is obtained from eqn (19), where $\Delta G = 0$. The line is curved because of the inverse proportional relationship between energy and wavelength ($E = hc/\lambda$).

There is a minimum E°_{ox} value required for any metal complex (with a particular co-reactant) to enable the possibility of ECL to occur *via* Scheme 1 ($\Delta G < 0$ for eqn (19)). Of the example metal complexes shown, only $[Ir(pmi)_3]$ (which does not generate co-reactant ECL with TPrA) does not meet this requirement.

In the 'catalytic route' depicted in Scheme 2 (reactions (10), (12) and (13)), we find a second condition on E°_{ox} of the metal complexes. This pathway may provide a more efficient[12] means to generate $\mathrm{TPrA}^{+\bullet}$, but will only proceed if the potential of the M/M^{+} couple is more positive than the oxidation potential of the co-reactant (Fig. 2). However, this is not an essential criterion for the generation of ECL, because $\mathrm{TPrA}^{+\bullet}$ is also electrochemically generated (reaction (11)). A well-known example of this is the co-reactant ECL of $[Ir(ppy)_3]$ (complex iii, Fig. 2), which cannot proceed with TPrA *via* this catalytic route, but still possesses a sufficient E°_{ox} to generate ECL *via* Scheme 1 (Fig. 1). In such cases, the reverse of reaction (12) may occur, where the $\mathrm{TPrA}^{+\bullet}$ species can oxidise the metal complex. Moreover, in cases were the E°_{ox} of the metal complex is sufficient to allow Scheme 2 to occur, its contribution to the overall ECL intensity will diminish as the concentration of the metal complex is lowered.[11]

The first reduction potential of the metal complex (E°_{red}) can also be an important factor in the relative intensity of co-reactant ECL. Although in aqueous solution it is generally difficult to reduce complexes such as $[Ru(bpy)_3]^{2+}$ at a platinum electrode, $[Ru(bpy)_3]^{+}$ has been detected when generated by other means and is sufficiently stable to produce ECL[12] *via* Scheme 3 (incorporating reactions (10), (11), (13), (15), (16) and (18)). For this to occur, the metal complex must be capable of being reduced by the $\mathrm{TPrA}^{\bullet}$ intermediate (reaction (15)).

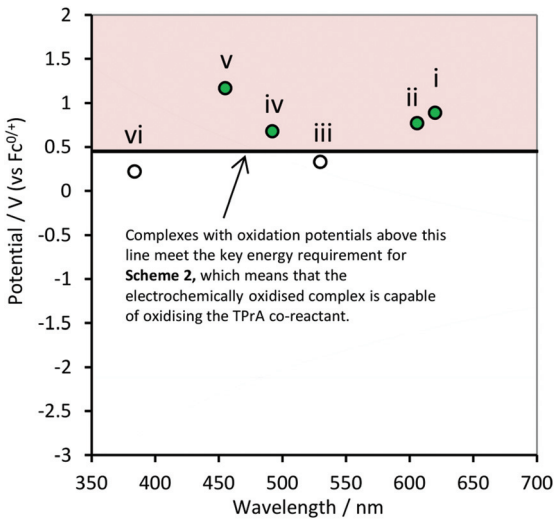


Fig. 2 Energy requirements for Scheme 2 (reaction (12)) with TPrA as co-reactant, in terms of oxidation potentials and emission wavelengths of the metal complexes: (i) $[Ru(bpy)_3]^{2+}$, (ii) $[Ir(ppy)_2(phen)]^{+}$, (iii) $[Ir(ppy)_3]$, (iv) $[Ir(df\text{-}ppy)_3]$, (v) $[Ir(df\text{-}ppy)_2(ptb)]^{+}$, and (vi) $[Ir(pmi)_3]$. Reaction (12) is energetically favourable for complexes with oxidation potentials above the line (in the red coloured area).

This journal is © The Royal Society of Chemistry 2016

Open Access Article. Published on 03 November 2015. Downloaded on 22/07/2016 16:53:49.
This article is licensed under a Creative Commons Attribution-NonCommercial 3.0 Unported Licence.

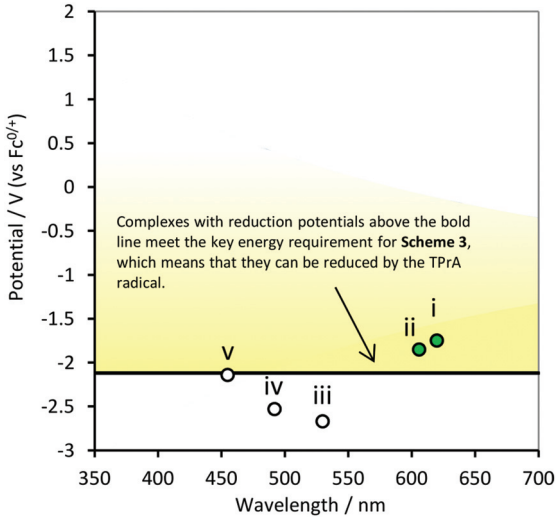


Fig. 3 Energy requirements for Scheme 3 (reaction (15)) with TPrA as co-reactant, in terms of reduction potentials and emission wavelengths of the metal complexes: (i) $[Ru(bpy)_3]^{2+}$, (ii) $[Ir(ppy)_2(phen)]^+$, (iii) $[Ir(ppy)_3]$, (iv) $[Ir(df\text{-}ppy)_3]$, and (v) $[Ir(df\text{-}ppy)_2(ptb)]^+$. Reaction (15) is energetically favourable for complexes with reduction potentials above the line (in the yellow coloured zone). The reduction potential of complex (vi) $[Ir(pmi)_3]$ is beyond the potential window of the solvent.

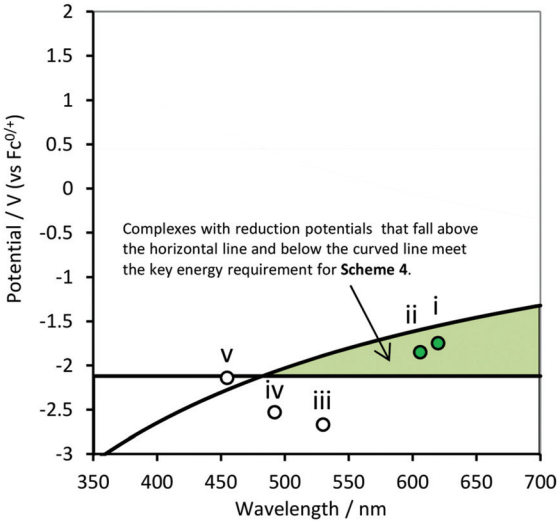


Fig. 4 Energy requirements for Scheme 4 (reactions (15) and (17)) with TPrA as co-reactant, in terms of reduction potentials and emission wavelengths of the metal complexes: (i) $[Ru(bpy)_3]^{2+}$, (ii) $[Ir(ppy)_2(phen)]^+$, (iii) $[Ir(ppy)_3]$, (iv) $[Ir(df\text{-}ppy)_3]$, (v) $[Ir(df\text{-}ppy)_2(ptb)]^+$, and (vi) $[Ir(pmi)_3]$. Reactions (15) and (17) are both energetically favourable for complexes with reduction potentials in the green coloured area. The reduction potential of complex (vi) $[Ir(pmi)_3]$ is beyond the potential window of the solvent. The curved line is obtained from eqn (20), where $\Delta G = 0$.

That is, the potential of the M/M^- couple must be less negative than that of $TPrA^{\bullet}$ (Fig. 3). Of the metal complexes shown, $[Ru(bpy)_3]^{2+}$ and $[Ir(ppy)_2(phen)]^+$ clearly meet this requirement, with $[Ir(df\text{-}ppy)_2(ptb)]^+$ a borderline case.

In 2002, Bard and co-workers provided evidence of another pathway in the co-reactant ECL of $[Ru(bpy)_3]^{2+}$ with TPrA, in which the emitter was generated by the reaction of $[Ru(bpy)_3]^+$ with $TPrA^{+\bullet}$ (Scheme 4, incorporating reactions: (11), (13), (15), (17) and (18)). This process is dependent on favourable energetics for both the formation of M^- (reaction (15)) and the subsequent generation of the excited state species upon reaction with $TPrA^{+\bullet}$ (reaction (17)). As with reaction (14), the energy required to generate the excited state in reaction (17) will be greater when the wavelength of emission is shorter, and can be estimated by the following relationship:

$$\Delta G = E^{\circ}(M^-) - E^{\circ}(TPrA^{\bullet+}) + E_{ES} \quad (20)$$

Only complexes with reduction potentials that fall into the enclosed zone shown in green in Fig. 4 will meet the energetic requirements of this pathway to ECL emission. Of the complexes shown, only $[Ru(bpy)_3]^{2+}$ and $[Ir(ppy)_2(phen)]^+$ are capable of generating ECL *via* Scheme 4.

Complexes for which the generation of M^- (reaction (15)) is energetically favourable (Fig. 3), irrespective of whether or not they can achieve the excited state *via* reaction with $TPrA^{+\bullet}$ (Fig. 4), can still generate the excited state species *via* the annihilation process (reaction (16)). However, at relatively low metal complex concentrations, the annihilation pathway will become less probable, and if energetically possible (*i.e.*, if the reduction potential of the metal complex falls into the green zone in Fig. 4), reaction (17) (Scheme 4) will become the dominant pathway to the excited state species from the reduced complex M^-.

Fig. 5 shows the combined energy requirements for Schemes 1–4 using TPrA as a co-reactant. It is clear that only one of the Ir^{III} complexes shown here, $[Ir(ppy)_2(phen)]^+$, can generate ECL *via* pathways analogous to all four schemes outlined by Bard and co-workers[13] for the classic $[Ru(bpy)_3]^{2+}$-TPrA system. This Ir^{III} complex was reported[17] to give a 4-fold greater co-reactant ECL intensity than $[Ru(bpy)_3]^{2+}$ under the same conditions.

Following Bard and co-workers' determination of the reduction potential of the $TPrA^{\bullet}$ radical,[28] Kim and co-workers[17] examined the co-reactant ECL of several Ir^{III} complexes that had reduction potentials less negative than $TPrA^{\bullet}$ and oxidation potentials more positive than $[Ir(ppy_3)]$ (which more importantly would mean that they were more positive than that of TPrA). These complexes included $[Ir(pq)_2(tmd)]$ (pq = 2-phenylquinoline anion; tmd = 2,2′,6,6′-tetramethylhepta-3,5-dione anion), and $[Ir(pq)_2(acac)]$ (acac = acetylacetonate anion), which gave co-reactant ECL intensities that were 49-fold and 77-fold greater than that of $[Ru(bpy)_3]^{2+}$, respectively. As shown in Fig. 6, the electrochemical and spectroscopic properties of these complexes facilitate reaction pathways analogous to all four schemes described by Bard and co-workers[13] for the generation of ECL.

Examining their respective positions in Fig. 6a, it is not immediately apparent why these two complexes gave much greater ECL intensities than similar complexes such as $[Ir(ppy)_2(phen)]^+$, which has a higher photoluminescence

Open Access Article. Published on 03 November 2015. Downloaded on 22/07/2016 16:53:49.
This article is licensed under a Creative Commons Attribution-NonCommercial 3.0 Unported Licence.

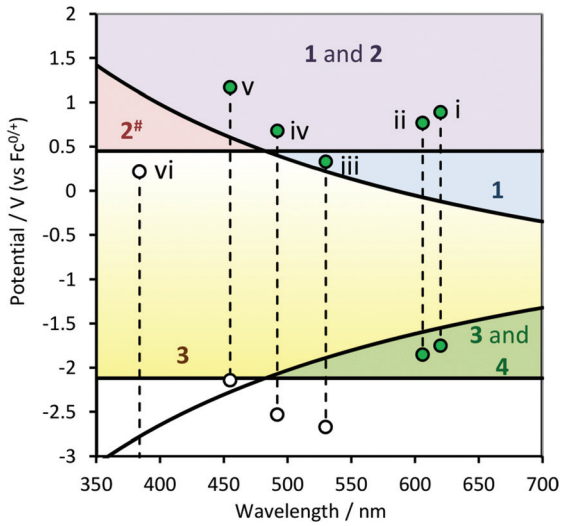


Fig. 5 Combined energy requirements for Schemes 1–4 (reactions (10)–(18)) with TPrA as co-reactant, in terms of redox potentials and emission wavelengths of the metal complexes: (i) $[Ru(bpy)_3]^{2+}$, (ii) $[Ir(ppy)_2(phen)]^+$, (iii) $[Ir(ppy)_3]$, (iv) $[Ir(df\text{-}ppy)_3]$, (v) $[Ir(df\text{-}ppy)_2(ptb)]^+$, and (vi) $[Ir(pmi)_3]$. The dashed lines link the oxidation and reduction potentials of each complex. The numbers indicate which schemes are feasible in each zone. #Scheme 2 results in the oxidation of TPrA, but the generation of ECL requires at least one of the other three schemes to occur.

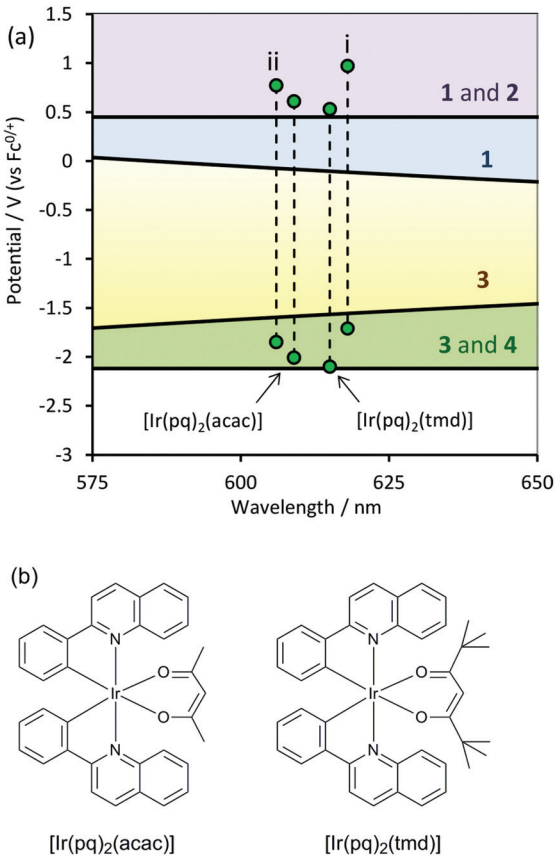


Fig. 6 (a) Position of the complexes reported by Kim and co-workers,[17] which exhibited excellent co-reactant ECL efficiencies with TPrA, in acetonitrile. Complexes: (i) $[Ru(bpy)_3]^{2+}$, and (ii) $[Ir(ppy)_2(phen)]^+$. The numbers on the right side of the graph indicate which schemes are energetically feasible in each zone. (b) Chemical structures of $[Ir(pq)_2(tmd)]$, and $[Ir(pq)_2(acac)]$, which gave co-reactant ECL with TPrA that was 49-fold and 77-fold greater than that of $[Ru(bpy)_3]^{2+}$ (in acetonitrile), respectively.

quantum yield (0.14 *vs.* 0.10). Kim *et al.*[17] ascribed the effectiveness of $[Ir(pq)_2(tmd)]$ and $[Ir(pq)_2(acac)]$ to "well-matched" oxidation and reduction potentials with those of TPrA and $TPrA^{\bullet}$, allowing efficient electron transfer, coupled with the high stability of the respective oxidation states of the complexes formed in the ECL process.

Fig. 5 also illustrates two major difficulties in developing blue-light emitters for efficient co-reactant ECL with TPrA: (a) as the emission energy increases, so does the M^+ potential required to generate the electronically excited M* upon reaction with $TPrA^{\bullet}$ (*i.e.*, the lower limit of purple zone in Fig. 5). This problem is compounded in aqueous solution, where this minimum oxidation potential quickly nears the level required to oxidise the solvent to dioxygen, which can quench the excited state. (b) For complexes with emission maxima below ~480 nm, even if it is possible to generate M^- (*via* reaction (15)), the reaction of M^- with $TPrA^{\bullet+}$ to produce M* (reaction (17)) is not energetically feasible (*i.e.*, left of green zone in Fig. 5), which removes Scheme 4 as a possible contributor to the overall ECL emission.

The negative charge on the ppy ligands of the green-ECL emitter $[Ir(ppy)_3]$ provides strong σ-donation through each Ir–C bond, resulting in facile metal-centred oxidation combined with difficult ligand based reduction. Consequently, as shown in Fig. 5, the only pathway to co-reactant ECL for $[Ir(ppy)_3]$ and TPrA is analogous to Scheme 1 (*i.e.*, the emitter is generated by reaction (14), but not reactions (16) and (17) under these circumstances). Not surprisingly, the co-reactant ECL of $[Ir(ppy)_3]$ with TPrA is poor compared to that of $[Ru(bpy)_3]^{2+}$,[22] despite its very high photoluminescence quantum yield.[18,22] The low redox potentials of $[Ir(ppy)_3]$ also result in its excited state being a particularly powerful reductant, which leads to the interesting and potentially useful quenching of its co-reactant ECL at high overpotentials.[24,25,30]

The presence of the electron withdrawing fluoro groups on the phenyl rings in $[Ir(df\text{-}ppy)_3]$ stabilises the HOMO and to a lesser extent the LUMO.[18] This not only results in a positive shift in both the oxidation and reduction potentials, but also a significant blue-shift in the emission. In terms of the energy requirements of the reaction pathways (Fig. 5), Schemes 1 and 2 are feasible for this complex, but not Schemes 3 and 4. The co-reactant ECL of $[Ir(df\text{-}ppy)_3]$ with TPrA is 5-fold greater than that of $[Ir(ppy)_3]$, but still considerably lower than that of $[Ru(bpy)_3]^{2+}$.

The replacement of a df-ppy with a 1-benzyl-1,2,3-triazol-4-ylpyridine (ptb) ligand, as in $[Ir(df\text{-}ppy)_2(ptb)]^+$, provides a further positive shift in redox potentials and blue-shift in the emission.[18] Therefore, reaction (14) becomes more energetically

 This journal is © The Royal Society of Chemistry 2016

Open Access Article. Published on 03 November 2015. Downloaded on 22/07/2016 16:53:49.
This article is licensed under a Creative Commons Attribution-NonCommercial 3.0 Unported Licence.

favourable, and as shown in Fig. 5, the reduction potential of this complex is now in a position that creates the possibility of a ECL pathway *via* the reduced M-complex (reactions (15) and (16)), analogous to Scheme 3. $[Ir(df\text{-}ppy)_2(ptb)]^+$ exhibits 3-fold superior co-reactant ECL intensity than $[Ir(df\text{-}ppy)_3]$, but still only 24% that of $[Ru(bpy)_3]^{2+}$ (with TPrA in acetonitrile).

The overall positive charge of $[Ir(df\text{-}ppy)_2(ptb)]^+$ provides greater solubility in polar solvents than neutral complexes such as $[Ir(ppy)_3]$ or $[Ir(df\text{-}ppy)_3]$,[18] but the aqueous solubility of $[Ir(df\text{-}ppy)_2(ptb)]^+$ is still much lower than $[Ru(bpy)_3]^{2+}$. Nevertheless, the combination of difluorophenylpyridine and triazolylpyridine ligands provides a good starting point for the development of efficient water-soluble blue-emitters for co-reactant ECL.[3,18]

We recently examined the relative co-reactant ECL intensity of two closely related complexes (Fig. 7b) that contained either a sulfonate group on each df-ppy ligand ($[Ir(df\text{-}ppy\text{-}SO_3)_2(ptb)]^-$) or a tetraethylene glycol (TEG) group on the triazolylpyridine ligand ($[Ir(df\text{-}ppy)_2(pt\text{-}TEG)]^+$) to further improve their aqueous solubility (Fig. 7b).[31] In buffered aqueous solution, with TPrA as co-reactant, these complexes gave ECL intensities that were 18% and 102% and that of $[Ru(bpy)_3]^{2+}$, respectively. The discrepancy between the ECL intensity of these two complexes is interesting, and may result from several contributing factors. Firstly, both complexes can proceed *via* pathways analogous to Schemes 1 and 2 (Fig. 7a), and as discussed above, Scheme 4 is not feasible. The parent $[Ir(df\text{-}ppy)_2(ptb)]^+$ was on the borderline of the reduction potential estimated for Scheme 3 (Fig. 3). Reduction potentials for $[Ir(df\text{-}ppy\text{-}SO_3)_2(ptb)]^-$ and $[Ir(df\text{-}ppy)_2(pt\text{-}TEG)]^+$ obtained in acetonitrile (100 μM complex with 0.1 M tetraammonium hexafluorophosphate) were found to be identical with that of $[Ir(df\text{-}ppy)_2(ptb)]^+$ (−2.14 V *vs.* $Fc^{0/+}$) within experimental error. Nevertheless, it should be noted that the M^- species generated in Scheme 3 will be less stable in water than acetonitrile (although it can contribute to the generation of ECL in either solvent[12]), and therefore even if feasible, Scheme 3 may make a lesser contribution in aqueous solution. Unlike the previous systems in acetonitrile, the oxidation of complexes in aqueous solution is to a certain extent compromised by the lower potential limit of the solvent, resulting in the generation of oxygen, which can quench the emission. Thus, the slightly higher applied potential required for the oxidation of $[Ir(df\text{-}ppy\text{-}SO_3)_2(ptb)]^-$ in aqueous solution could be expected to lower its ECL intensity relative to $[Ir(df\text{-}ppy)_2(pt\text{-}TEG)]^+$. However, it is perhaps more likely that the observed difference in ECL intensity arises from the inherent relative stabilities of the corresponding M^+ forms of the complexes in that solvent.

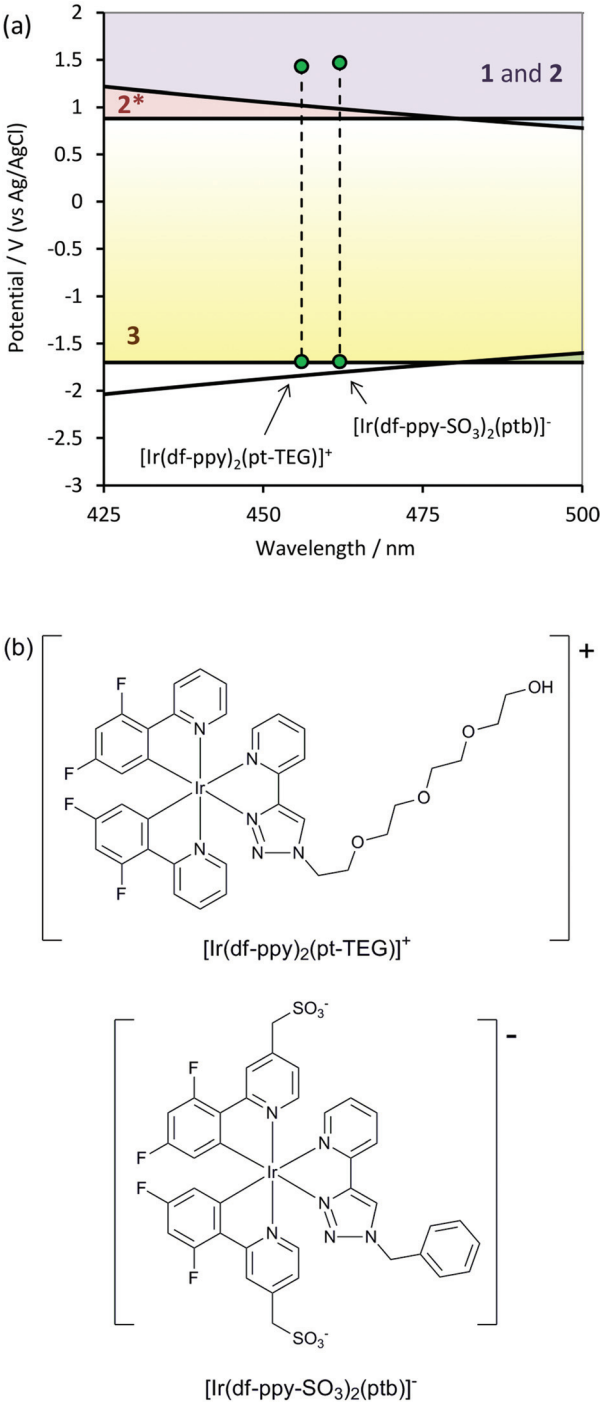


Fig. 7 (a) Position of two Ir^{III} complexes exhibiting high aqueous solubility and reasonably high blue ECL intensities with TPrA as co-reactant in buffered aqueous solution.[31] The reduction potential were estimated based on measurements in acetonitrile solvent. (b) Chemical structures of $[Ir(df\text{-}ppy)_2(pt\text{-}TEG)]^+$, and $[Ir(df\text{-}ppy\text{-}SO_3)_2(ptb)]^-$, which gave co-reactant ECL with TPrA that was 102% and 18% that of $[Ru(bpy)_3]^{2+}$ (in buffered aqueous solution), respectively.

Other considerations

It is important to discuss the limitations of these graphs. Their construction depends on the accuracy of the electrochemical and spectroscopic data. The redox potentials of the metal complex are generally easy to measure, but that of irreversibly oxidised co-reactants, and short lived intermediates such as $TPrA^{\bullet}$, are difficult to establish and will inevitably carry some error. Moreover, redox potentials often vary with

Open Access Article. Published on 03 November 2015. Downloaded on 22/07/2016 16:53:49.
This article is licensed under a Creative Commons Attribution-NonCommercial 3.0 Unported Licence.

conditions such as pH,[12] solvent,[12] and electrode material,[11] which (coupled with variation in reported reference electrode potentials[32]) can make it difficult to directly compare data between different studies.

The emission maxima of the complexes are ideally taken from low-temperature data, but this is not always available, and so room temperature data may be used as an approximation. Differences in the λ_{max} of Ir^{III} complexes established at 298 K and 77 K of 5–15 nm are common.[19]

Significant error in reported λ_{max} can arise due to a lack of correction for the sensitivity of the spectrometer and/or photodetector over the wavelength range. This effect can also introduce considerable bias into comparisons of the relative ECL intensities of complexes with significantly different emission maxima. For example, using a 'blue sensitive' bialkali photomultiplier tube, we recently measured the overall ECL intensity of the blue-emitter $[Ir(df\text{-}ppy)_2(pt\text{-}TEG)]^+$ as 12-fold greater than that of the orange-emitter $[Ru(bpy)_3]^{2+}$ under the same conditions (using TPrA as a co-reactant).[31] However, when we replaced the photomultiplier tube with an 'extended-range' trialkali analogue, the measured ECL intensity of $[Ir(df\text{-}ppy)_2(pt\text{-}TEG)]^+$ was only 0.4-fold that of the Ru^{II} complex.

Care must also be taken in the interpretation of these graphs. They provide a useful guide of the energy required for several key reaction steps for complexes that emit different wavelengths of light, and a quick assessment of the feasible reaction pathways. However, they do not directly account for factors such as the stability of the oxidised and reduced complexes, the kinetics of the reactions, luminescence quantum yields, influence of the potential window of the solvent, the effect of the electrode material on electrochemical reaction steps, and possible quenching of the excited state by the various species in solution,[12,30] which can have a major influence on the ECL intensity.

Nevertheless, these graphs can serve as guide to the development of new analytical ECL systems, especially where consideration of the light-producing pathways is an important factor. For example, in typical commercial ECL-based immunodiagnostic systems, the metal-complex labels in the immunoassay are immobilised on magnetic microbeads. Even when the beads are held to the electrode by a magnetic field, most of the metal complexes will not be close enough to the electrode for direct oxidation[13] and therefore Scheme 4 becomes a critical pathway to realise highly sensitive ECL detection under these conditions. Fig. 4 indicates that this pathway is not feasible for metal complexes exhibiting blue luminescence when TPrA is used as a co-reactant. Finally, this approach (Fig. 1–5) highlights the importance of discovering new co-reactants that best compliment the electrochemical characteristics of novel electrochemiluminophores.

References

1 *Electrogenerated Chemiluminescence*, ed. A. J. Bard, Marcel Dekker, New York, 2004.
2 R. Y. Lai, X. Kong, S. A. Jenekhe and A. J. Bard, *J. Am. Chem. Soc.*, 2003, **125**, 12631–12639; I.-S. Shin, S. Yoon, J. I. Kim, J.-K. Lee, T. H. Kim and H. Kim, *Electrochim. Acta*, 2011, **56**, 6219–6223; K. N. Swanick, M. Sandroni, Z. Ding and E. Zysman-Colman, *Chem. – Eur. J.*, 2015, **21**, 7435–7440.
3 S. Zanarini, M. Felici, G. Valenti, M. Marcaccio, L. Prodi, S. Bonacchi, P. Contreras-Carballada, R. M. Williams, M. C. Feiters, R. J. M. Nolte, L. De Cola and F. Paolucci, *Chem. – Eur. J.*, 2011, **17**, 4640–4647.
4 E. Kerr, E. H. Doeven, G. J. Barbante, C. F. Hogan, D. Bower, P. S. Donnelly, T. U. Connell and P. S. Francis, *Chem. Sci.*, 2015, **6**, 472–479.
5 T. Nobeshima, M. Nakakomi, K. Nakamura and N. Kobayashi, *Adv. Opt. Mater.*, 2013, **1**, 144–149; H. C. Moon, T. P. Lodge and C. D. Frisbie, *J. Am. Chem. Soc.*, 2014, **136**, 3705–3712.
6 M.-M. Chang, T. Saji and A. J. Bard, *J. Am. Chem. Soc.*, 1977, **99**, 5399–5403.
7 I. Rubinstein and A. J. Bard, *J. Am. Chem. Soc.*, 1981, **103**, 512–516.
8 J. K. Leland and M. J. Powell, *J. Electrochem. Soc.*, 1990, **137**, 3127–3131.
9 W. Miao, *Chem. Rev.*, 2008, **108**, 2506–2553.
10 X. Zhou, D. Zhu, Y. Liao, W. Liu, H. Liu, Z. Ma and D. Xing, *Nat. Protocols*, 2014, **9**, 1146–1159.
11 Y. Zu and A. J. Bard, *Anal. Chem.*, 2000, **72**, 3223–3232.
12 F. Kanoufi, Y. Zu and A. J. Bard, *J. Phys. Chem. B*, 2001, **105**, 210–216.
13 W. Miao, J.-P. Choi and A. J. Bard, *J. Am. Chem. Soc.*, 2002, **124**, 14478–14485.
14 C. M. Hindson, G. R. Hanson, P. S. Francis, J. L. Adcock and N. W. Barnett, *Chem. – Eur. J.*, 2011, **17**, 8018–8022.
15 M. M. Richter, *Chem. Rev.*, 2004, **104**, 3003–3036; R. Pyati and M. M. Richter, *Annu. Rep. Prog. Chem., Sect. C: Phys. Chem.*, 2007, **103**, 12–78; L. Hu and G. Xu, *Chem. Soc. Rev.*, 2010, **39**, 3275–3304; Y. Yuan, S. Han, L. Hu, S. Parveen and G. Xu, *Electrochim. Acta*, 2012, **82**, 484–492; K. Muzyka, *Biosens. Bioelectron.*, 2014, **54**, 393–407.
16 L. Xue, L. Guo, B. Qiu, Z. Lin and G. Chen, *Electrochem. Commun.*, 2009, **11**, 1579–1582; J. L. Delaney, C. F. Hogan, J. Tian and W. Shen, *Anal. Chem.*, 2011, **83**, 1300–1306.
17 J. I. Kim, I.-S. Shin, H. Kim and J.-K. Lee, *J. Am. Chem. Soc.*, 2005, **127**, 1614–1615.
18 G. J. Barbante, E. H. Doeven, E. Kerr, T. U. Connell, P. S. Donnelly, J. M. White, T. Lópes, S. Laird, C. F. Hogan, D. J. D. Wilson, P. J. Barnard and P. S. Francis, *Chem. – Eur. J.*, 2014, **20**, 3322–3332.
19 L. Flamigni, A. Barbieri, C. Sabatini, B. Ventura and F. Barigelletti, *Top. Curr. Chem.*, 2007, **281**, 143–203.
20 R. J. Forster, P. Bertoncello and T. E. Keyes, *Annu. Rev. Anal. Chem.*, 2009, **2**, 359–385.
21 A. Kapturkiewicz and G. Angulo, *Dalton Trans.*, 2003, 3907–3913.
22 D. Bruce and M. M. Richter, *Anal. Chem.*, 2002, **74**, 1340–1342.

 This journal is © The Royal Society of Chemistry 2016

Open Access Article. Published on 03 November 2015. Downloaded on 22/07/2016 16:53:49.
This article is licensed under a Creative Commons Attribution-NonCommercial 3.0 Unported Licence.



23 B. D. Muegge and M. M. Richter, *Anal. Chem.*, 2004, **76**, 73–77; E. H. Doeven, E. M. Zammit, G. J. Barbante, C. F. Hogan, N. W. Barnett and P. S. Francis, *Angew. Chem., Int. Ed.*, 2012, **51**, 4354–4357.
24 E. H. Doeven, E. M. Zammit, G. J. Barbante, P. S. Francis, N. W. Barnett and C. F. Hogan, *Chem. Sci.*, 2013, **4**, 977–982; E. H. Doeven, G. J. Barbante, E. Kerr, C. F. Hogan, J. A. Endler and P. S. Francis, *Anal. Chem.*, 2014, **86**, 2727–2732.
25 E. H. Doeven, G. J. Barbante, C. F. Hogan and P. S. Francis, *ChemPlusChem*, 2015, **80**, 456–470.
26 H. J. Bolink, L. Cappelli, E. Coronado, M. Grätzel, E. Orti, R. D. Costa, P. M. Viruela and M. K. Nazeeruddin, *J. Am. Chem. Soc.*, 2006, **128**, 14786–14787; H. Lin, M. E. Cinar and M. Schmittel, *Dalton Trans.*, 2010, **39**, 5130–5138; R. V. Kiran, C. F. Hogan, B. D. James and D. J. D. Wilson, *Eur. J. Inorg. Chem.*, 2011, 4816–4825.
27 W. E. Geiger, *Organometallics*, 2007, **26**, 5738–5765.
28 R. Y. Lai and A. J. Bard, *J. Phys. Chem. A*, 2003, **107**, 3335–3340.
29 B. D. Stringer, L. M. Quan, P. J. Barnard, D. J. D. Wilson and C. F. Hogan, *Organometallics*, 2014, **33**, 4860–4872; G. J. Barbante, E. H. Doeven, P. S. Francis, B. D. Stringer, C. F. Hogan, P. R. Kheradmand, D. J. D. Wilson and P. J. Barnard, *Dalton Trans.*, 2015, **44**, 8564–8576.
30 G. J. Barbante, N. Kebede, C. M. Hindson, E. H. Doeven, E. M. Zammit, G. R. Hanson, C. F. Hogan and P. S. Francis, *Chem. – Eur. J.*, 2014, **20**, 14026–14031.
31 E. Kerr, E. H. Doeven, G. J. Barbante, T. U. Connell, P. S. Donnelly, D. J. D. Wilson, T. D. Ashton, F. M. Pfeffer and P. S. Francis, *Chem. – Eur. J.*, 2015, **21**, 14987–14995.
32 V. V. Pavlishchuk and A. W. Addison, *Inorg. Chim. Acta*, 2000, **298**, 97–102.